Latin American Journal of Solids and Structures
www.lajss.org

# Free Vibration Analysis of Orthtropic Thin Cylindrical Shells with Variable Thickness by Using Spline Functions

**Abstract**

In this study, vibration behavior of orthotropic cylindrical shells with variable thickness is investigated. Based on linear shell theory and applying energy method and using spline functions, free vibration relations are derived for shell with variable thickness and curvature. Frequency parameter and mode shapes are found after solving the frequency Eigenvalue equation. Effects of variable thickness along axial and circumferential directions of the shell on its frequency parameter are studied and compared against each other. Shell thickness is assumed to be varied in a parabolic profile along both directions. Also, frequency parameters for both circular and parabolic curvatures along circumferential direction are investigated and results are compared together. In addition, effect of variable thickness on the mode shapes is studied.

**Keywords**

Cylindrical shell, Parabolic curvature, Variable thickness, Natural frequency, Spline function, Discrete method.

**Pouria Bahrami Ataabadi**[a]
**Mohammad Reza Khedmati**[* a]
**Mostafa Bahrami Ataabadi**[b]

[a] Department of Marine Technology, Amirkabir University of Technology, 424 Hafez Avenue, Tehran 15916-34311, Iran
[b] Department of Engineering and Building, National Iranian Oil Company, Boushehr, 3rd Pars 75391-154, Iran

[*]Author email: khedmati@aut.ac.ir

Received 15.05.2014
In revised form 29.06.2014
Accepted 18.08.2014
Available online 26.09.2014

## 1 INTRODUCTION

Cylindrical (open) shells with either circular or noncircular profiles have been widely used in recent years, as structural elements within marine, civil, aerospace, and petrochemical industries. In addition, because of inherent difficulties in assembly of shells with circular profile, noncircular profile is preferred in constructing cylindrical shells. Vibration behavior of cylindrical shells with circular profile is different than that of cylindrical shells with noncircular profile.

Variation of the thickness in a cylindrical shell leads to decrease of its structural weight besides reducing cost of needed materials. Moreover, natural frequency of the shell changes as a result of its variable thickness. Therefore, vibration analysis of the shells with variable thickness has attracted the attention of many researchers in recent years.

Zhang *et al.* (2001) and Pellicano (2007) studied vibration behavior of the shells incorporating circular profile and uniform thickness. A few other researchers have also studied vibration response of noncircular shells, among them are Srinivasan and Bobby (1976), Cheung and Cheung (1972) and Yamada *et al.* (1999).

Vibration response of flat plates with variable thickness has also been addressed by Huang *et al.* (2005, 2007), Ashour (2001), Sakiyama and Huang (1998), Grigorenko *et al.* (2008). On the other hand, Sivadas and Ganesan (1991), Zhang and Xiang (2006), Duan and Koh (2008) investigated vibration response of the closed shells having circular profiles and variable thickness. Their investigations were limited to the effects of variable thickness in one direction (either axial or circumferential) on vibration behavior of the shells. Later, Grigorenko and Parkhomenko (2011) studied free vibration of shallow shells having parabolically-variable thickness with the aid of spline-collocation approach. The effects of variable thickness on the vibration behavior of closed elliptical cylindrical shells and closed oval cylindrical shells have been studied by Suzuki and Leissa (1985) and Khalifa (2011), respectively.

Open parabolic cylindrical shell with variable thickness is considered as the main geometry in the present study. As it was shown, very few research works have been performed on such structures. In addition, vibration response of parabolic cylindrical shells and circular cylindrical shells are compared against each other's. As it was mentioned earlier, most of the previous works studied the effects of thickness variation in one direction on the vibration response of the shells. Therefore, a thorough study on the effects of direction of thickness variation on the vibration response of a shell is lacked herein. Present work is aimed at study of vibration response for both parabolic shells and circular shells having variable thickness in either axial direction or circumferential direction.
On the other hand, analytical solutions cannot be simply reached for assessment of vibration response of the shells when both radius and thickness are subjected to variation. Thus, numerical approaches as well as approximate methods may be used to investigate the vibration response of these types of the shells. Techniques based on spline functions are among numerical methods that are useful in solving structural problems. In the present work, a relatively simple discrete method incorporating spline functions introduced already by Cheng and Chuang (1990) and Cheng *et al.* (1987) for shell and plate with uniform thickness and uniform curvature; is further extended to be able to analyze free vibrations of circular/noncircular cylindrical shells with variable thickness.

The aims of present work are: (1) to extend discrete method based on the concept of spline functions for studying vibration behavior of parabolic and circular cylindrical shells with non-uniform distribution of thickness and to prove its efficiency and accuracy, (2) to evaluate the effects of thickness variation along the axis of the shell on its natural frequency in comparison with those of thickness variation along the circumference of the shell on its natural frequency, (3) to compare natural frequency of cylindrical shells having circular profile with that of cylindrical shells having parabolic profile; and finally, (4) to investigate the effects of thickness variation on the mode shapes of the shells.

## 2 THEORY AND FORMULATIONS

Since thickness of the shell is small compared to its other dimensions, the shell is regarded to be thin. Consequently, classical shell theory based on Kirchhoff–Love assumptions is used to extract governing equations.

### 2.1 Geometric formulation

The main geometry under consideration in this work is a cylindrical shell with an either circular or parabolic profile. Both circular and parabolic profiles can be defined by two parameters including camber (C) and span (b), Figure 1. Geometrical relations for circular and parabolic profiles are given in Table 1.

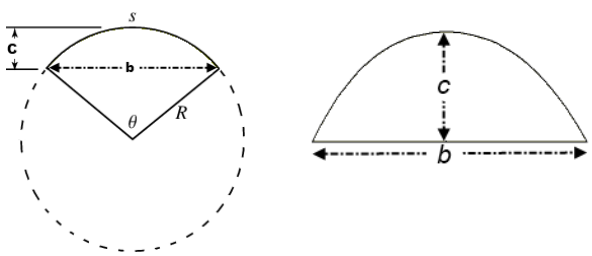


(a) (b)

**Figure 1:** (a) circular profile and (b) parabolic profile.

Figure 2 shows a shell with a parabolic profile in the curvilinear coordinate system (xsz). z-axis is perpendicular to the middle surface of shell defined by x-s plane. x-axis is along axis of the cylinder, while the s-axis is along circumference of the cylinder. Displacement functions along x-axis, s-axis and z-axis are respectively represented by U(x,s), V(x,s) and W(x,s). Lame's parameters for this type of shell in the curvilinear coordinate system are equal to one according to Soedel (1993).

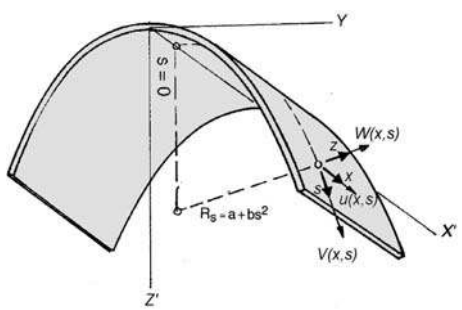


**Figure 2:** Parabolic cylindrical shell, curvilinear coordinate system (xsz) and displacement functions (Soedel (1993)).

### 2.2. Displacement functions

Displacement functions for the middle surface of the shell are introduced by cubic and fifth-order B-spline functions as below.

$$\begin{aligned} \mathrm{U}(\mathrm{x},\mathrm{s}) &= \lfloor \phi(\mathrm{x}) \rfloor \otimes \lfloor \phi(\mathrm{s}) \rfloor \{\mathrm{A}\} \sin(\omega \mathrm{t} + \mathrm{e}) \\ \mathrm{V}(\mathrm{x},\mathrm{s}) &= \lfloor \phi(x) \rfloor \otimes \lfloor \phi(\mathrm{s}) \rfloor \{\mathrm{B}\} \sin(\omega \mathrm{t} + \mathrm{e}) \\ \mathrm{W}(\mathrm{x},\mathrm{s}) &= \lfloor \varphi(\mathrm{x}) \rfloor \otimes \lfloor \varphi(\mathrm{s}) \rfloor \{\mathrm{C}\} \sin(\omega \mathrm{t} + \mathrm{e}) \end{aligned} \tag{1}$$

Row matrices $\lfloor \phi(x) \rfloor$ and $\lfloor \varphi(x) \rfloor$ are cubic B-spline and fifth-order B-spline matrices, respectively. Column matrices $\{A\}, \{B\}$ and $\{C\}$ are unknown coefficients of the displacement functions in Equation 1. Also, N is the number of divisions along x or s axes. The operator $\otimes$ is the 'Kronecker product' of the matrices. Formulations of row matrices and also column matrices are given below

$$\begin{aligned} \lfloor \phi(\mathrm{x}) \rfloor &= \left[ \phi(\mathrm{x})_{-1}\ \phi(\mathrm{x})_0\ \phi(\mathrm{x})_1 \ldots\ldots \phi(\mathrm{x})_{\mathrm{N}-1}\ \phi(\mathrm{x})_{\mathrm{N}}\ \phi(\mathrm{x})_{\mathrm{N}+1} \right]_{\mathrm{N}+3} \\ \lfloor \varphi(\mathrm{x}) \rfloor &= \left[ \psi(\mathrm{x})_{-2}\ \psi(\mathrm{x})_{-1}\ \psi(\mathrm{x})_0 \ldots\ldots \psi(\mathrm{x})_{\mathrm{N}}\ \psi(\mathrm{x})_{\mathrm{N}+1}\ \psi(\mathrm{x})_{\mathrm{N}+2} \right]_{\mathrm{N}+5} \\ \{\mathrm{A}\}^{\mathrm{T}} &= \left[ \{\mathrm{a}_{-1}\}^{\mathrm{T}} \{\mathrm{a}_0\}^{\mathrm{T}} \ldots\ldots \{\mathrm{a}_{\mathrm{N}}\}^{\mathrm{T}} \{\mathrm{a}_{\mathrm{N}+1}\}^{\mathrm{T}} \right]_{[(\mathrm{N}+3)]} \\ \{\mathrm{a_i}\}^{\mathrm{T}} &= \left[ \mathrm{a_{i1}}\ \mathrm{a_{i2}}\ \mathrm{a_{i3}} \ldots\ldots \mathrm{a_{iN}} \right], \mathrm{i} = -1,0,1,\ldots \mathrm{N}+1 \quad , \{B\}\ is\ same\ as \{\mathrm{A}\} \\ \{\mathrm{C}\}^{\mathrm{T}} &= \left[ \{\mathrm{c}_{-2}\}^{\mathrm{T}} \{\mathrm{c}_{-1}\}^{\mathrm{T}} \ldots\ldots \{\mathrm{c}_{\mathrm{N}+1}\}^{\mathrm{T}} \{\mathrm{c}_{\mathrm{N}+2}\}^{\mathrm{T}} \right]_{[(\mathrm{N}+5)]} \\ \{\mathrm{c_i}\}^{\mathrm{T}} &= \left[ \mathrm{c_{i1}}\ \mathrm{c_{i2}}\ \mathrm{c_{i3}} \ldots\ldots \mathrm{c_{iN}} \right], \mathrm{i} = -2,-1,0,\ldots \mathrm{N}+2 \end{aligned} \tag{2}$$

Standard cubic spline is expressed as

$$\varphi_3(\mathrm{x}) = \frac{1}{6} \begin{cases} (2+\mathrm{x})^3 & \mathrm{x} \in [-2,-1] \\ (2+\mathrm{x})^3 - 4(1+\mathrm{x})^3 & \mathrm{x} \in [-1,0] \\ (2-\mathrm{x})^3 - 4(1-\mathrm{x})^3 & \mathrm{x} \in [0,1] \\ (2-\mathrm{x})^3 & \mathrm{x} \in [1,2] \\ 0 & |\mathrm{x}| > 2 \end{cases} \tag{3}$$

According to Cheng *et al.* (1987), cubic B-spline functions ($B_3$) for N equal divisions (N>4) are

$$\begin{aligned} \phi_{\mathrm{i}} &= \varphi_3\left(\frac{\mathrm{x}}{\mathrm{h}} - \mathrm{i}\right), \mathrm{i} = 3,4,5\ldots,\mathrm{N}-3 \\ \phi_{-1} &= \varphi_3\left(\frac{\mathrm{x}}{\mathrm{h}} + 1\right) & \phi_{\mathrm{N}-2} &= \varphi_3\left(\frac{\mathrm{x}}{\mathrm{h}} - \mathrm{N} + 2\right) \\ \phi_0 &= \varphi_3\left(\frac{\mathrm{x}}{\mathrm{h}}\right) - 4\varphi_3\left(\frac{\mathrm{x}}{\mathrm{h}} + 1\right) & \phi_{\mathrm{N}-1} &= \varphi_3\left(\frac{\mathrm{x}}{\mathrm{h}} - \mathrm{N} + 1\right) - \frac{1}{2}\varphi_3\left(\frac{\mathrm{x}}{\mathrm{h}} - \mathrm{N}\right) + \varphi_3\left(\frac{\mathrm{x}}{\mathrm{h}} - \mathrm{N} - 1\right) \\ \phi_1 &= \varphi_3\left(\frac{\mathrm{x}}{\mathrm{h}} - 1\right) - \frac{1}{2}\varphi_3\left(\frac{\mathrm{x}}{\mathrm{h}}\right) + \varphi_3\left(\frac{\mathrm{x}}{\mathrm{h}} + 1\right) & \phi_{\mathrm{N}} &= \varphi_3\left(\frac{\mathrm{x}}{\mathrm{h}} - \mathrm{N}\right) - 4\varphi_3\left(\frac{\mathrm{x}}{\mathrm{h}} - \mathrm{N} - 1\right) \\ \phi_2 &= \varphi_3\left(\frac{\mathrm{x}}{\mathrm{h}} - 2\right) & \phi_{\mathrm{N}+1} &= \varphi_3\left(\frac{\mathrm{x}}{\mathrm{h}} - \mathrm{N} - 1\right) \end{aligned} \tag{4}$$

Expression for the standard fifth-order spline is

$$\varphi_5 = \frac{1}{120}\begin{cases} \left(3+x\right)^5 & x \in \left[-3,-2\right] \\ \left(3+x\right)^5 - 6\left(2+x\right)^5 & x \in \left[-2,-1\right] \\ \left(3+x\right)^5 - 6\left(2+x\right)^5 + 15\left(1+x\right)^5 & x \in \left[-1,0\right] \\ \left(3-x\right)^5 - 6\left(2-x\right)^5 + 15\left(1-x\right)^5 & x \in \left[0,1\right] \\ \left(3-x\right)^5 - 6\left(2-x\right)^5 & x \in \left[1,2\right] \\ \left(3-x\right)^5 & x \in \left[2,3\right] \\ 0 & \left|x\right| > 3 \end{cases} \tag{5}$$

Again, according to Cheng *et al.* (1987), fifth-order B-spline functions ($B_5$) for N equal divisions (N>6) are

$$\begin{aligned} \psi_i &= \varphi_5\left(\frac{x}{h} - i\right), i = 4,5,6\ldots N-4 \\ \psi_{-2} &= \varphi_5\left(\frac{x}{h} + 2\right) \\ \psi_{-1} &= \varphi_5\left(\frac{x}{h} + 1\right) - 26\varphi_5\left(\frac{x}{h} + 2\right) \\ \psi_0 &= \alpha_{11}\varphi_5\left(\frac{x}{h} + 2\right) + \alpha_{12}\varphi_5\left(\frac{x}{h} + 1\right) + \varphi_5\left(\frac{x}{h}\right) \\ \psi_1 &= \alpha_{21}\varphi_5\left(\frac{x}{h} + 1\right) + \alpha_{22}\varphi_5\left(\frac{x}{h}\right) + \varphi_5\left(\frac{x}{h} - 1\right) \\ \psi_2 &= \alpha_{31}\varphi_5\left(\frac{x}{h} + 2\right) + \alpha_{32}\varphi_5\left(\frac{x}{h}\right) + \varphi_5\left(\frac{x}{h} - 2\right) \\ \psi_3 &= \varphi_5\left(\frac{x}{h} - 3\right) \\ \psi_{N-3} &= \varphi_5\left(\frac{x}{h} - N + 3\right) \\ \psi_{N-2} &= \beta_{31}\varphi_5\left(\frac{x}{h} - N + 2\right) + \beta_{32}\varphi_5\left(\frac{x}{h} - N\right) + \varphi_5\left(\frac{x}{h} - N - 2\right) \\ \psi_{N-1} &= \beta_{21}\varphi_5\left(\frac{x}{h} - N - 1\right) + \beta_{22}\varphi_5\left(\frac{x}{h} - N\right) + \varphi_5\left(\frac{x}{h} - N + 1\right) \\ \psi_N &= \beta_{11}\varphi_5\left(\frac{x}{h} - N - 2\right) + \beta_{12}\varphi_5\left(\frac{x}{h} - N - 1\right) + \varphi_5\left(\frac{x}{h} - N\right) \\ \psi_{N+1} &= \varphi_5\left(\frac{x}{h} - N - 1\right) + 26\varphi_5\left(\frac{x}{h} - N - 2\right) \\ \psi_{N+2} &= \varphi_5\left(\frac{x}{h} - N - 2\right) \end{aligned} \tag{6}$$

where, for cc boundary condition (clamped edges at x=0, x=L)

$$\begin{bmatrix} \alpha_{11} & \alpha_{12} \\ \alpha_{21} & \alpha_{22} \\ \alpha_{31} & \alpha_{32} \end{bmatrix} = \begin{bmatrix} \beta_{11} & \beta_{12} \\ \beta_{21} & \beta_{22} \\ \beta_{31} & \beta_{32} \end{bmatrix} = \begin{bmatrix} 165/4 & -33/8 \\ 1 & -26/33 \\ 1 & -1/33 \end{bmatrix}$$

And for ss boundary condition (simply supported edges at x=0, x=L)

$$\begin{bmatrix} \alpha_{11} & \alpha_{12} \\ \alpha_{21} & \alpha_{22} \\ \alpha_{31} & \alpha_{32} \end{bmatrix} = \begin{bmatrix} \beta_{11} & \beta_{12} \\ \beta_{21} & \beta_{22} \\ \beta_{31} & \beta_{32} \end{bmatrix} = \begin{bmatrix} 12 & -3 \\ -1 & 0 \\ -1 & 0 \end{bmatrix}$$

### 2.3 Mass and stiffness matrices

Extracted relations in this section are valid only for a shell with a general geometry.

#### 2.3.1 Mass matrix

Kinetic energy of a shell with variable thickness can be expressed in the following form

$$T_{shell} = \frac{1}{2}\iint \rho_{shell} t_{shell} \left(U^2 + V^2 + W^2\right) dxds = \frac{1}{2}\{\delta\}^T [M]\{\delta\} \tag{7}$$

where, $\rho_{shell}$ is density, $t_{shell}$ is thickness function of shell, U, V and W are displacement functions of the middle surface of shell. Also, $\{\delta\} = \left[\{A\}\ \{B\}\ \{C\}\right]^T$, where $\{A\}$, $\{B\}$ and $\{C\}$ are unknown coefficients of displacement functions. $[M]$ is also mass matrix.

After substituting the displacement functions (Equation 1) into the Equation 7 and taking numerical integration, the mass matrix is obtained by equation 8. This mass matrix is for a shell with variable thickness in x-direction. Through replacing x by s, the mass matrix for a shell with variable thickness in s-direction can be easily obtained.

$$[M] = \rho_{shell} \begin{bmatrix} (F_{tx} \otimes F_s) & 0 & 0 \\ 0 & (F_{tx} \otimes F_s) & 0 \\ 0 & 0 & (H_{tx} \otimes H_s) \end{bmatrix} \tag{8}$$

#### 2.3.2 Stiffness matrix

Strain energy for a shell with a general geometry can be written as follows

$$U_{shell} = \frac{1}{2}\iint \{\varepsilon\}^T [D]\{\varepsilon\}\, dxds = \frac{1}{2}\{\delta\}^T [K]\{\delta\} \tag{9}$$

where, the strain vector is

$$\{\varepsilon\} = \begin{bmatrix} \varepsilon_1 & \varepsilon_2 & \gamma_{12} & \chi_1 & \chi_2 & \chi_{12} \end{bmatrix}$$

The components of strain vector are

$$\begin{cases} \varepsilon_1 = \dfrac{1}{A_1}\dfrac{U}{\partial x} + \dfrac{1}{A_1 A_2}\dfrac{\partial A_1}{\partial s}V + \dfrac{W}{R_1} \\ \varepsilon_2 = \dfrac{1}{A_2}\dfrac{V}{\partial s} + \dfrac{1}{A_1 A_2}\dfrac{\partial A_2}{\partial x}U + \dfrac{W}{R_2} \\ \gamma_{12} = \dfrac{A_2}{A_1}\dfrac{\partial}{\partial s}\left(\dfrac{U}{A_2}\right) + \dfrac{A_1}{A_2}\dfrac{\partial}{\partial s}\left(\dfrac{V}{A_1}\right) \\ \chi_1 = -\left[\dfrac{1}{A_1}\dfrac{\partial}{\partial x}\left(\dfrac{U}{R_1} + \dfrac{1}{A_1}\dfrac{\partial W}{\partial x}\right) + \dfrac{1}{A_1 A_2}\dfrac{\partial A_1}{\partial s}\left(\dfrac{V}{R_2} + \dfrac{1}{A_2}\dfrac{\partial W}{\partial s}\right)\right] \\ \chi_2 = -\left[\dfrac{1}{A_2}\dfrac{\partial}{\partial s}\left(\dfrac{V}{R_2} + \dfrac{1}{A_2}\dfrac{\partial W}{\partial s}\right) + \dfrac{1}{A_1 A_2}\dfrac{\partial A_2}{\partial x}\left(\dfrac{U}{R_1} + \dfrac{1}{A_1}\dfrac{\partial W}{\partial x}\right)\right] \\ \chi_{12} = -\left[\dfrac{1}{A_1 A_2}\left(-\dfrac{1}{A_1}\dfrac{\partial A_1}{\partial s}\dfrac{\partial W}{\partial x} - \dfrac{1}{A_2}\dfrac{\partial A_2}{\partial x}\dfrac{\partial W}{\partial s} + \dfrac{\partial^2 W}{\partial x \partial s}\right) + \dfrac{1}{R_1}\dfrac{A_1}{A_2}\dfrac{\partial}{\partial s}\left(\dfrac{U}{A_1}\right) + \dfrac{1}{R_2}\dfrac{A_2}{A_1}\dfrac{\partial}{\partial x}\left(\dfrac{V}{A_2}\right)\right] \\ W, U, V \text{ are displacement functions} \\ R_1 \text{is radius of curvature along } X - \text{axis} \\ R_2 \text{is radius of curvature along } S - \text{axis} \\ A_1, A_2 \text{are Lame}' \text{ parameters} \end{cases}$$

Flexural rigidity of the shell is given as

$$[D] = \begin{bmatrix} B_{11}(x,s) & B_{12}(x,s) & 0 & 0 & 0 & 0 \\ B_{21}(x,s) & B_{22}(x,s) & 0 & 0 & 0 & 0 \\ 0 & 0 & B_{66}(x,s) & 0 & 0 & 0 \\ 0 & 0 & 0 & D_{11}(x,s) & D_{12}(x,s) & 0 \\ 0 & 0 & 0 & D_{21}(x,s) & D_{22}(x,s) & 0 \\ 0 & 0 & 0 & 0 & 0 & D_{66}(x,s) \end{bmatrix}$$

$$\begin{cases} B_{ii}(x,s) = \dfrac{E_i t(x,s)}{1 - \vartheta_i \vartheta_j} \quad , \; D_{ij}(x,s) = \vartheta_j D_{ii}(x,s) & E_i \; is \; elastic \; modulus \\ B_{ij}(x,s) = \vartheta_j B_{ii}(x,s) \quad , \quad B_{66} = G_{ij} t(x,s) & G_{ij} \; is \; shear \; modulus \\ D_{ii}(x,s) = \dfrac{B_{ii} t^2(x,s)}{12} \quad , \; D_{66} = \dfrac{B_{66} t^2(x,s)}{6} & t(x,s) \; is \; thickness \; function \\ & \vartheta_j \; is \; poisson's \; ratio \end{cases}$$

Stiffness matrix $[K]$ is

$$[K] = \begin{bmatrix} k_{11} & k_{12} & k_{13} \\ k_{21} & k_{22} & k_{23} \\ k_{31} & k_{32} & k_{33} \end{bmatrix}, \qquad k_{21} = k_{12}^T, k_{31} = k_{13}^T, k_{32} = k_{23}^T$$

After substituting displacement functions from the Equation 1 into the Equation 9 and taking an integration of it, components of stiffness matrix are obtained as follows

$$
\begin{aligned}
k_{11} &= \left[\left(\frac{E_1}{1-\vartheta_1\vartheta_2}\right)D_{tx}\otimes F_s + G_{12}\left(F_{tx}\otimes D_s\right)\right]\\
k_{12} &= \left[\vartheta_2\left(\frac{E_1}{1-\vartheta_1\vartheta_2}\right)E_{tx}^{T}\otimes E_s + G_{12}\left(E_{tx}\otimes E_s^{T}\right)\right]\\
k_{13} &= \left[\left(\vartheta_2+1\right)\left(\frac{E_1}{1-\vartheta_1\vartheta_2}\right)L_{tRx}^{T}\otimes G_s^{T}\right]\\
k_{22} &= \left[\left(\frac{E_2}{1-\vartheta_1\vartheta_2}\right)F_{tx}\otimes D_s + G_{12}\left(D_{tx}\otimes F_s\right)\right]\\
k_{23} &= \left[\left(\vartheta_1+1\right)\left(\frac{E_2}{1-\vartheta_1\vartheta_2}\right)G_{tx}^{T}\otimes G_{Rs}^{T}\right]\\
k_{33} &= \left[\begin{array}{l}\left(\frac{E_1}{1-\vartheta_1\vartheta_2}\right)\left(1+\vartheta_1\right)H_{tx}\otimes H_{RRs} + \left(\frac{E_2}{1-\vartheta_1\vartheta_2}\right)\left(1+\vartheta_2\right)H_{tRx}\otimes H_s\\ +\vartheta_1\left(\frac{E_2}{12\left(1-\vartheta_1\vartheta_2\right)}\right)J_{tttx}\otimes J_s^{T} + \left(\frac{E_1}{12\left(1-\vartheta_1\vartheta_2\right)}\right)K_{tttx}\otimes H_s\\ +\vartheta_2\left(\frac{E_1}{12\left(1-\vartheta_1\vartheta_2\right)}\right)J_{tttx}^{T}\otimes J_s + \frac{G_{12}}{6}I_{tttx}\otimes I_s + \left(\frac{E_2}{12\left(1-\vartheta_1\vartheta_2\right)}\right)H_{tttx}\otimes K_s\end{array}\right]
\end{aligned}
\tag{10}
$$

Some matrices are available in the list of the elements in the formulations of mass and stiffness matrices, which are called as spline matrices. Some of these spline matrices have been already derived by Cheng *et al.* (1987), while other spline matrices representing the effect of variable radius and thickness are extracted herein. Formulations of all spline matrices are presented in Table 2 and Table 3.

| | | |
|---|---|---|
| $F_x = \int_0^L \left\lfloor \phi(x)\right\rfloor^T \left\lfloor \phi(x)\right\rfloor dx$ | $L_x = \int_0^L \left\lfloor \varphi(x)\right\rfloor^T \left\lfloor \phi'(x)\right\rfloor dx$ | $I_x = \int_0^L \left\lfloor \varphi'(x)\right\rfloor^T \left\lfloor \varphi'(x)\right\rfloor dx$ |
| $G_x = \int_0^L \left\lfloor \varphi(x)\right\rfloor^T \left\lfloor \phi(x)\right\rfloor dx$ | $D_x = \int_0^L \left\lfloor \phi'(x)\right\rfloor^T \left\lfloor \phi'(x)\right\rfloor dx$ | $J_x = \int_0^L \left\lfloor \varphi(x)\right\rfloor^T \left\lfloor \varphi''(x)\right\rfloor dx$ |
| $K_x = \int_0^L \left\lfloor \varphi''(x)\right\rfloor^T \left\lfloor \varphi''(x)\right\rfloor dx$ | $H_x = \int_0^L \left\lfloor \varphi(x)\right\rfloor^T \left\lfloor \varphi(x)\right\rfloor dx$ | $E_x = \int_0^L \left\lfloor \phi(x)\right\rfloor^T \left\lfloor \phi'(x)\right\rfloor dx$ |
| $Z_x = \int_0^L \left\lfloor \varphi'(x)\right\rfloor^T \left\lfloor \phi(x)\right\rfloor dx$ | | $S_x = \int_0^L \left\lfloor \varphi''(x)\right\rfloor^T \left\lfloor \varphi'(x)\right\rfloor dx$ |

Note: Through replacing x by s in these relations, spline matrices in s direction can be obtained.

**Table 2:** Spline matrices used in this study and also the study of Cheng *et al.* (1987).

## 2.4 Frequency equation

Total potential energy for free vibration of a shell is expressed as follows

$$\Pi = \frac{2\pi}{\omega}\left[\left\{\delta\right\}^T\left(\left[K\right]-\omega^2\left[M\right]\right)\left\{\delta\right\}\right] \tag{11}$$

Substituting mass and stiffness matrices into the above equation and using the Hamilton's principle, following form of the frequency equation is obtained.

$$\left(\left[\mathrm{K}\right]-\omega^2\left[\mathrm{M}\right]\right)\left\{\delta\right\}=0 \tag{12}$$

Equation 12 is of eigenvalue type in which the eigenvalues represent the natural frequencies. Unknown coefficients of displacement functions create the eigenvectors. Solving the Equation 12 will result in the frequencies and corresponding mode shapes.

| | | |
|---|---|---|
| $F_{tx}=\int_0^L t(x)\left\lfloor\phi(x)\right\rfloor^T\left\lfloor\phi(x)\right\rfloor dx$ | $L_{Rs}=\int_0^b \left\lfloor\varphi(s)\right\rfloor^T\left\lfloor\phi'(s)\right\rfloor ds$ | $L_{tx}=\int_0^L t(x)\left\lfloor\varphi(x)\right\rfloor^T\left\lfloor\phi'(x)\right\rfloor dx$ |
| $I_{tttx}=\int_0^L t^3(x)\left\lfloor\varphi'(x)\right\rfloor^T\left\lfloor\varphi'(x)\right\rfloor dx$ | $G_{Rs}=\int_0^b \frac{\left\lfloor\varphi(s)\right\rfloor^T\left\lfloor\phi(s)\right\rfloor}{R_s} ds$ | $G_{tx}=\int_0^L t(x)\left\lfloor\varphi(x)\right\rfloor^T\left\lfloor\phi(x)\right\rfloor dx$ |
| $D_{tx}=\int_0^L t(x)\left\lfloor\phi'(x)\right\rfloor^T\left\lfloor\phi'(x)\right\rfloor dx$ | $J_{Rs}=\int_0^b \frac{\left\lfloor\varphi(s)\right\rfloor^T\left\lfloor\varphi''(s)\right\rfloor}{R_s} ds$ | $J_{tttx}=\int_0^L t^3(x)\left\lfloor\varphi(x)\right\rfloor^T\left\lfloor\varphi''(x)\right\rfloor dx$ |
| $H_{RRs}=\int_0^b \frac{\left\lfloor\varphi(s)\right\rfloor^T\left\lfloor\varphi(s)\right\rfloor}{R_s^2} ds$ | $H_{Rs}=\int_0^b \frac{\left\lfloor\varphi(s)\right\rfloor^T\left\lfloor\varphi(s)\right\rfloor}{R_s} ds$ | $H_{tx}=\int_0^L t(x)\left\lfloor\varphi(x)\right\rfloor^T\left\lfloor\varphi(x)\right\rfloor dx$ |
| $K_{tttx}=\int_0^L t^3(x)\left\lfloor\varphi''(x)\right\rfloor^T\left\lfloor\varphi''(x)\right\rfloor dx$ | | $E_{tx}=\int_0^L t(x)\left\lfloor\phi(x)\right\rfloor^T\left\lfloor\phi'(x)\right\rfloor dx$ |

Note: Through replacing x by s in matrices, spline matrices in s direction can be obtained.

**Table 3:** Spline matrices extracted in this study.

## 3 NUMERICAL EXAMPLES AND DISCUSSIONS

Based on derived formulations in the previous section, a code was written in the MATLAB environment in order to calculate the natural frequencies and also corresponding mode shapes.

### 3.1 Verification of present method

Accuracy of presented formulations is investigated in this section in order to demonstrate its ability to analyze free vibration of both parabolic and circular cylindrical shells with either uniform or variable thickness. A comparison between natural frequencies for a circular cylindrical shell having a uniform thickness as obtained by the present method and also by Srinivasan and Bobby (1976) is given in Table 4. It should be mentioned that Srinivasan and Bobby (1976) used Rayleigh–Ritz and matrix methods in their work. On the other hand, natural frequencies as obtained by the present method and the method developed by Cheung and Cheung (1972) are provided in Table 5 for a parabolic cylindrical shell with a constant thickness. Cheung and Cheung (1972) used strip method to extract relations for vibration analysis of a cylindrical shell with parabolic profile. In Table 6 results of the present method have been compared with those of Huang *et al.* (2005) who used dis-

crete method in combination with Green's function to obtain natural frequency solution for flat plates with variable thickness in one direction. Table 7 shows frequency parameters for a shallow shell with rectangular platform that its thickness varies parabolically in one direction (Grigorenko and Parkhomenko (2011)). Grigorenko and Parkhomenko (2011) obtained their solution method by using spline-collocation method.

| Mode number | Present work | | | Petyt as reported in Srinivasan and Bobby (1976) | | Difference (%) |
|---|---|---|---|---|---|---|
| | Mesh Divisions | | | Analysis Method | | |
| | $12\times12$ | $14\times14$ | $16\times16$ | Extended Rayleigh-Ritz | Finite element | $100\left(\frac{\omega^{16\times16}-\omega^{\mathrm{Ref.[3]}}}{\omega^{\mathrm{Ref.[3]}}}\right)$ |
| $1^{st}$ | 882 | 879 | 876 | 870 | 870 | -0.68 |
| $2^{nd}$ | 959 | 957 | 955 | 958 | 958 | 0.31 |
| $3^{rd}$ | 1297 | 1284 | 1282 | 1288 | 1288 | 0.46 |
| $4^{th}$ | 1369 | 1367 | 1366 | 1364 | 1363 | -0.14 |
| $5^{th}$ | 1446 | 1444 | 1443 | 1440 | 1440 | -0.20 |

$\mathrm{E}=1.0\mathrm{e}7\,lb/in^2, \mathrm{R_s}=30\mathrm{in}, \vartheta=0.33, \mathrm{a}=3\mathrm{in}, \mathrm{b}=4\mathrm{in}, \mathrm{thickness}=0.013, \rho=0.0002484\,lbs^2/in^2, \mathrm{B.c}=\mathrm{CCCC}$

**Table 4:** Natural frequencies (Hz) for a circular cylindrical shell model (Srinivasan and Bobby (1976)).

| Mode number | Present Study | | | Cheung and Cheung (1972) | Difference (%) |
|---|---|---|---|---|---|
| | Mesh Divisions | | | | |
| | $12\times12$ | $14\times14$ | $16\times16$ | | $100\left(\frac{\omega^{16\times16}-\omega^{\mathrm{Ref.[4]}}}{\omega^{\mathrm{Ref.[4]}}}\right)$ |
| $1^{st}$ | 0.30914 | 0.307773 | 0.30552 | 0.303 | 0.831683 |
| $2^{nd}$ | 0.30722 | 0.307101 | 0.30668 | 0.306 | 0.222222 |
| $3^{rd}$ | 0.56179 | 0.558907 | 0.55264 | 0.537 | 2.912477 |
| $4^{th}$ | 0.54222 | 0.539315 | 0.53974 | 0.538 | 0.32342 |
| $5^{th}$ | 0.56934 | 0.568532 | 0.56844 | 0.571 | -0.44834 |

$\mathrm{E}=1, \vartheta=0.3, \mathrm{a}=1\mathrm{in}, \mathrm{b}=1\mathrm{in}, \mathrm{thickness}=0.191\mathrm{in}, \rho=1, \mathrm{B.c}=\mathrm{SSSS}$

**Table 5:** Natural frequencies (Rad/sec) for a parabolic cylindrical shell model (Cheung and Cheung (1972)).

| | $b/a=1.0$ | | | $b/a=0.5$ | | |
|---|---|---|---|---|---|---|
| Frequency parameter | $\alpha$ | | | $\alpha$ | | |
| | 0.00 | 0.40 | 0.80 | 0.00 | 0.40 | 0.80 |
| $\lambda_1^{\text{Present work}}$ | 6.765 | 7.386 | 7.897 | 10.256 | 11.147 | 11.954 |
| $\lambda_1^{\text{Huang et al. (2005)}}$ | 6.780 | 7.402 | 7.945 | 10.194 | 11.113 | 11.894 |
| Difference (%) | -0.22 | -0.21 | -0.60 | 0.60 | 0.30 | 0.50 |
| $\lambda_2^{\text{Present work}}$ | 8.944 | 9.708 | 10.468 | 12.171 | 13.286 | 14.386 |
| $\lambda_2^{\text{Huang et al.(2005)}}$ | 8.953 | 9.770 | 10.475 | 12.289 | 13.422 | 14.419 |
| Difference (%) | -0.10 | -0.63 | -0.06 | -0.96 | -1.01 | -0.22 |
| $\lambda_3^{\text{Present work}}$ | 10.305 | 11.217 | 12.050 | 15.270 | 16.587 | 17.862 |
| $\lambda_3^{\text{Huang et al. (2005)}}$ | 10.293 | 11.232 | 12.046 | 15.301 | 16.695 | 17.908 |
| Difference (%) | 0.11 | -0.13 | 0.03 | -0.20 | -0.64 | -0.25 |
| $\lambda_4^{\text{Present work}}$ | 11.511 | 12.532 | 13.475 | 16.246 | 17.563 | 18.434 |
| $\lambda_4^{\text{Huang et al. (2005)}}$ | 11.615 | 12.679 | 13.610 | 16.131 | 17.476 | 18.511 |
| Difference (%) | -0.89 | -1.15 | -0.99 | 0.71 | 0.49 | -0.41 |

$$E_1 = 60.7e9pa, E_2 = 24.8e9pa, R_s = \infty, \vartheta_{12} = 0.23, h_0 = 0.01a, B.C = CCCC$$

$$\text{flat plate thickness} = h_0\left(1+\alpha x/a\right), \lambda_i = \rho h_0 \omega_i^2 a^4 \Big/ \left[D_0\left(1-\vartheta_{21}\vartheta_{12}\right)\right]$$

$$D_0 = E_2 h_0^3 \Big/ \left[12\left(1-\vartheta_{21}\vartheta_{12}\right)\right],\ \ Difference = 100\left(\lambda^{present\ work} - \lambda^{Ref}\right)/\lambda^{Ref}$$

**Table 6:** Dimensionless frequency parameter for a flat plate with variable thickness in one direction (Huang *et al.* (2005)).

| Frequency parameter | $\alpha=-0.4, BC1$ | | | | | $\alpha=0.4, BC2$ | | | | |
|---|---|---|---|---|---|---|---|---|---|---|
| $\lambda$ | $12\times12$ | $14\times14$ | $16\times16$ | $18\times18$ | $20\times20$ | $12\times12$ | $14\times14$ | $16\times16$ | $18\times18$ | $20\times20$ |
| $\lambda_1^{\text{Present work}}$ | 15.58 | 15.57 | 15.57 | 15.56 | 15.56 | 29.58 | 29.55 | 29.53 | 29.53 | 29.52 |
| $\lambda_1^{\text{Grigorenko (2011)}}$ | 16.65 | 16.12 | 15.75 | 15.73 | 15.71 | 30.55 | 30.26 | 30.12 | 29.85 | 29.78 |
| Difference (%) | -6.42 | -3.41 | -1.14 | -1.08 | -0.95 | -3.17 | -2.34 | -1.95 | -1.07 | -0.87 |
| $\lambda_2^{\text{Present work}}$ | 37.95 | 37.81 | 37.74 | 37.70 | 37.68 | 48.32 | 48.05 | 47.92 | 47.85 | 47.81 |
| $\lambda_2^{\text{Grigorenko (2011)}}$ | 38.36 | 37.99 | 37.44 | 37.34 | 37.33 | 49.32 | 48.64 | 48.43 | 48.09 | 47.91 |
| Difference (%) | -1.06 | -0.47 | 0.80 | 0.96 | 0.93 | -2.02 | -1.21 | -1.05 | -0.49 | -0.20 |
| $\lambda_3^{\text{Present work}}$ | 38.90 | 38.90 | 38.89 | 38.89 | 38.89 | 56.13 | 56.12 | 56.12 | 56.11 | 56.11 |
| $\lambda_3^{\text{Grigorenko (2011)}}$ | 40.06 | 39.58 | 39.25 | 39.13 | 38.97 | 58.66 | 57.52 | 57.36 | 57.02 | 56.96 |
| Difference | -2.89 | -1.71 | -0.91 | -0.61 | -0.20 | -4.31 | -2.43 | -2.16 | -1.59 | -1.49 |
| $\lambda_4^{\text{Present work}}$ | 54.18 | 54.09 | 54.04 | 54.01 | 54.00 | 70.75 | 70.59 | 70.52 | 70.48 | 70.46 |
| $\lambda_4^{\text{Grigorenko (2011)}}$ | 54.40 | 54.35 | 54.28 | 54.23 | 54.19 | 71.76 | 71.44 | 71.16 | 70.87 | 70.81 |
| Difference | -0.40 | -0.47 | -0.44 | -0.40 | -0.35 | -1.4 | -1.1 | -0.89 | -0.55 | -0.49 |

$$E_1 = 3.68e10pa, E_2 = 2.68e10pa, G_{12} = 0.5e10pa, R_s = 12.5, R_x = 12.5, \vartheta_{12} = 0.077, h_0 = 0.04$$

$$, BC1: CCCC, BC2: SSSS, h\left(x\right) = h_0\left(\alpha\left(6x^2-6x+1\right)+1\right)$$

$$\lambda_i = \omega_i a^2\sqrt{\rho h_0 \Big/ D_{11}}, D_{11} = E_1 h_0^3 \Big/ \left[12\left(1-\vartheta_{21}\vartheta_{12}\right)\right],\ \ Difference = 100\left[\lambda^{present\ work} - \lambda^{Ref}\right]\Big/\lambda^{Ref}$$

**Table 7:** Dimensionless frequency parameter for a shallow shell with variable thickness in one direction (Grigorenko and Parkhomenko (2011)).

It is observed that present solution method is in sufficient agreement with the studies performed by above-mentioned researchers. Comparison results have shown the accuracy of present solution method for analyzing vibration of shells. In parallel, a convergence study was performed during the comparison analyses, based on which the number of divisions in both directions was defined to be equal to 16 for all examples.

| Model ID | Profile | Geometrical properties of model | Mechanical properties of material | B.c | Thickness function |
|---|---|---|---|---|---|
| M1x | Circular | $\text{camber}(c) = 0.05\text{m}$<br>$\text{span of shell}(b) = 1\text{m}$<br>$\text{lenght of shell}(a) = 1\text{m}$ | $E_x = 3.68\text{e}10\text{Pa}$<br>$E_s = 2.68\text{e}10\text{Pa}$<br>$G_{xs} = 0.50\text{e}10\text{Pa}$<br>$\vartheta_{xs} = 0.077$ | B.c1<br>B.c2<br>B.c3 | Thickness function 1 |
| M1s | | | | | Thickness function 2 |
| M2x | Circular | $\text{camber}(c) = 0.1\text{m}$<br>$\text{span of shell}(b) = 1\text{m}$<br>$\text{lenght of shell}(a) = 1\text{m}$ | $E_x = 3.68\text{e}10\text{Pa}$<br>$E_s = 2.68\text{e}10\text{Pa}$<br>$G_{xs} = 0.50\text{e}10\text{Pa}$<br>$\vartheta_{xs} = 0.077$ | B.c1<br>B.c2<br>B.c3 | Thickness function 1 |
| M2s | | | | | Thickness function 2 |
| M3x | Circular | $\text{camber}(c) = 0.15\text{m}$<br>$\text{span of shell}(b) = 1\text{m}$<br>$\text{lenght of shell}(a) = 1\text{m}$ | $E_x = 3.68\text{e}10\text{Pa}$<br>$E_s = 2.68\text{e}10\text{Pa}$<br>$G_{xs} = 0.50\text{e}10\text{Pa}$<br>$\vartheta_{xs} = 0.077$ | B.c1<br>B.c2<br>B.c3 | Thickness function 1 |
| M3s | | | | | Thickness function 2 |
| M4x | parabolic | $\text{camber}(c) = 0.05\text{m}$<br>$\text{span of shell}(b) = 1\text{m}$<br>$\text{lenght of shell}(a) = 1\text{m}$ | $E_x = 3.68\text{e}10\text{Pa}$<br>$E_s = 2.68\text{e}10\text{Pa}$<br>$G_{xs} = 0.50\text{e}10\text{Pa}$<br>$\vartheta_{xs} = 0.077$ | B.c1<br>B.c2<br>B.c3 | Thickness function 1 |
| M4s | | | | | Thickness function 2 |
| M5x | parabolic | $\text{camber}(c) = 0.1\text{m}$<br>$\text{span of shell}(b) = 1\text{m}$<br>$\text{lenght of shell}(a) = 1\text{m}$ | $E_x = 3.68\text{e}10\text{Pa}$<br>$E_s = 2.68\text{e}10\text{Pa}$<br>$G_{xs} = 0.50\text{e}10\text{Pa}$<br>$\vartheta_{xs} = 0.077$ | B.c1<br>B.c2<br>B.c3 | Thickness function 1 |
| M5s | | | | | Thickness function 2 |
| M6x | parabolic | $\text{camber}(c) = 0.15\text{m}$<br>$\text{span of shell}(b) = 1\text{m}$<br>$\text{lenght of shell}(a) = 1\text{m}$ | $E_x = 3.68\text{e}10\text{Pa}$<br>$E_s = 2.68\text{e}10\text{Pa}$<br>$G_{xs} = 0.50\text{e}10\text{Pa}$<br>$\vartheta_{xs} = 0.077$ | B.c1<br>B.c2<br>B.c3 | Thickness function 1 |
| M6s | | | | | Thickness function 2 |

MNx: model with variable thickness in x direction.
MNs: model with variable thickness in s direction.
B.c1=CCCC, B.c2=SSSS and B.c3=CSCS (x=0, a are clamped, s=0,b are simply supported).
$\alpha$, in thickness function, is called thickness parameter that varies between -0.4 and 0.4

$$\text{Thickness function 1 is } h(x) = h_0\left[1+\alpha\left(1+6\left(x^2/a^2\right)-6\left(x/a\right)\right)\right]$$

$$\text{Thickness function 2 is } h(s) = h_0\left[1+\alpha\left(1+6\left(s^2/b^2\right)-6\left(s/b\right)\right)\right]$$

**Table 8:** General characteristics for the studied models.

### 3.2 Vibration analysis

In this section, vibration of circular and parabolic cylindrical panels having variable thicknesses along their circumferences or axes is studied. Three sets of the models with circular profile and also three more sets of the models with parabolic profile are constructed. Besides, each set has two subsets of the models with variable thicknesses. One subset is corresponding to the models having variable thicknesses along their circumferences (represented by MNs), while the other subset is including the models with variable thicknesses along their axes (represented by MNx). For each of the subsets, three cases for the boundary conditions are considered. General characteristics for all investigated models are introduced in Table 8. Variation of frequency parameter against thickness parameter (α) is presented in Tables 9-11 for the case of circular models. Frequency parameter for the models having a variable thickness along their axis varies in a manner completely reverse to that of the models having variable thickness along their circumference for the BC1 boundary conditions.

| Model ID: M1 | | $\alpha$ | | | | | | | | |
|---|---|---|---|---|---|---|---|---|---|---|
| Boundary conditions | λ | -0.4 | -0.3 | -0.2 | -0.1 | 0 | 0.1 | 0.2 | 0.3 | 0.4 |
| BC1 | $\lambda_1^{M1s}$ | 12.200 | 12.448 | 12.671 | 12.871 | 13.104 | 13.203 | 13.337 | 13.448 | 13.538 |
| | $\lambda_1^{M1x}$ | 13.953 | 13.754 | 13.546 | 13.334 | 13.120 | 12.907 | 12.698 | 12.493 | 12.296 |
| | $\lambda_2^{M1s}$ | 13.610 | 13.880 | 14.233 | 14.472 | 14.650 | 14.722 | 14.935 | 15.031 | 15.123 |
| | $\lambda_2^{M1x}$ | 14.763 | 14.741 | 14.717 | 14.689 | 14.655 | 14.616 | 14.568 | 14.511 | 14.440 |
| | $\lambda_3^{M1s}$ | 18.039 | 18.138 | 18.196 | 18.202 | 18.064 | 17.917 | 17.775 | 17.634 | 17.496 |
| | $\lambda_3^{M1x}$ | 17.330 | 17.500 | 17.653 | 17.790 | 17.992 | 18.019 | 18.111 | 18.188 | 18.213 |
| | $\lambda_4^{M1s}$ | 18.598 | 18.474 | 18.341 | 18.233 | 18.244 | 18.231 | 18.193 | 18.132 | 18.046 |
| | $\lambda_4^{M1x}$ | 17.774 | 17.923 | 18.040 | 18.128 | 18.209 | 18.229 | 18.244 | 18.239 | 18.250 |
| BC2 | $\lambda_1^{M1s}$ | 5.797 | 5.895 | 5.990 | 6.084 | 6.177 | 6.273 | 6.371 | 6.473 | 6.581 |
| | $\lambda_1^{M1x}$ | 5.743 | 5.856 | 5.969 | 6.075 | 6.177 | 6.278 | 6.380 | 6.483 | 6.588 |
| | $\lambda_2^{M1s}$ | 8.224 | 8.293 | 8.324 | 8.324 | 8.309 | 8.244 | 8.171 | 8.079 | 7.969 |
| | $\lambda_2^{M1x}$ | 8.929 | 8.783 | 8.635 | 8.490 | 8.318 | 8.212 | 8.084 | 7.964 | 7.856 |
| | $\lambda_3^{M1s}$ | 12.169 | 12.214 | 12.256 | 12.297 | 12.311 | 12.391 | 12.446 | 12.428 | 12.365 |
| | $\lambda_3^{M1x}$ | 11.984 | 12.117 | 12.211 | 12.261 | 12.308 | 12.318 | 12.307 | 12.276 | 12.227 |
| | $\lambda_4^{M1s}$ | 12.431 | 12.499 | 12.537 | 12.550 | 12.543 | 12.518 | 12.479 | 12.510 | 12.583 |
| | $\lambda_4^{M1x}$ | 12.431 | 12.496 | 12.533 | 12.550 | 12.550 | 12.537 | 12.512 | 12.478 | 12.436 |
| BC3 | $\lambda_1^{M1s}$ | 7.304 | 7.339 | 7.375 | 7.415 | 7.461 | 7.513 | 7.574 | 7.644 | 7.725 |
| | $\lambda_1^{M1x}$ | 6.504 | 6.731 | 6.941 | 7.179 | 7.461 | 7.624 | 7.850 | 8.079 | 8.308 |
| | $\lambda_2^{M1s}$ | 9.158 | 9.220 | 9.245 | 9.242 | 9.232 | 9.161 | 9.089 | 9.003 | 8.896 |
| | $\lambda_2^{M1x}$ | 9.554 | 9.476 | 9.398 | 9.322 | 9.250 | 9.182 | 9.120 | 9.065 | 9.017 |
| | $\lambda_3^{M1s}$ | 14.939 | 14.989 | 15.007 | 14.979 | 14.844 | 14.810 | 14.731 | 14.657 | 14.592 |
| | $\lambda_3^{M1x}$ | 13.569 | 13.864 | 14.136 | 14.385 | 14.794 | 14.826 | 15.020 | 15.199 | 15.322 |
| | $\lambda_4^{M1s}$ | 15.193 | 15.134 | 15.060 | 14.999 | 14.970 | 14.922 | 14.860 | 14.782 | 14.694 |
| | $\lambda_4^{M1x}$ | 14.208 | 14.432 | 14.626 | 14.795 | 14.971 | 15.065 | 15.170 | 15.255 | 15.361 |

$$\lambda_i = \omega_i a^2 \left(\rho h_0 / D_{11}\right)^{0.5}, D_{11} = E_1 h_0^3 / [12(1 - \vartheta_{21}\vartheta_{12})]$$

**Table 9:** Variation of natural frequency parameter for M1x and M1s models.

In addition, it is observed that variation of first frequency parameter against the thickness parameter is linear upwards or downwards for both of the models having variable thickness along their axis or circumference for the BC1 boundary conditions.

| Model ID: M2 | | $\alpha$ | | | | | | | | |
|---|---|---|---|---|---|---|---|---|---|---|
| Boundary conditions | $\lambda$ | -0.4 | -0.3 | -0.2 | -0.1 | 0 | 0.1 | 0.2 | 0.3 | 0.4 |
| BC1 | $\lambda_1^{M2s}$ | 14.379 | 14.478 | 14.56 | 14.619 | 14.643 | 14.776 | 14.822 | 14.854 | 14.872 |
| | $\lambda_1^{M2x}$ | 14.766 | 14.723 | 14.692 | 14.661 | 14.644 | 14.583 | 14.571 | 14.569 | 14.528 |
| | $\lambda_2^{M2s}$ | 18.007 | 18.402 | 18.752 | 19.062 | 19.112 | 19.570 | 19.772 | 19.942 | 20.077 |
| | $\lambda_2^{M2x}$ | 19.882 | 19.662 | 19.548 | 19.481 | 19.113 | 18.68 | 18.245 | 17.878 | 17.543 |
| | $\lambda_3^{M2s}$ | 22.478 | 22.421 | 22.341 | 22.243 | 21.917 | 21.990 | 21.837 | 21.666 | 21.475 |
| | $\lambda_3^{M2x}$ | 21.223 | 21.407 | 21.553 | 21.697 | 21.909 | 21.976 | 22.040 | 22.082 | 22.144 |
| | $\lambda_4^{M2s}$ | 24.017 | 24.114 | 24.180 | 24.220 | 24.235 | 24.227 | 24.197 | 24.146 | 24.072 |
| | $\lambda_4^{M2x}$ | 23.937 | 24.070 | 24.163 | 24.216 | 24.234 | 24.220 | 24.168 | 24.098 | 23.9 |
| BC2 | $\lambda_1^{M2s}$ | 8.971 | 9.046 | 9.087 | 9.098 | 9.0759 | 9.0512 | 8.998 | 8.927 | 8.842 |
| | $\lambda_1^{M2x}$ | 9.395 | 9.308 | 9.223 | 9.147 | 9.062 | 8.992 | 8.947 | 8.891 | 8.862 |
| | $\lambda_2^{M2s}$ | 10.121 | 10.357 | 10.585 | 10.807 | 11.027 | 11.248 | 11.469 | 11.693 | 11.922 |
| | $\lambda_2^{M2x}$ | 10.024 | 10.292 | 10.547 | 10.794 | 11.025 | 11.254 | 11.470 | 11.693 | 11.915 |
| | $\lambda_3^{M2s}$ | 15.229 | 15.347 | 15.431 | 15.486 | 15.497 | 15.529 | 15.522 | 15.501 | 15.465 |
| | $\lambda_3^{M2x}$ | 15.133 | 15.263 | 15.35 | 15.428 | 15.493 | 15.521 | 15.530 | 15.382 | 15.031 |
| | $\lambda_4^{M2s}$ | 15.989 | 16.127 | 16.200 | 16.221 | 16.195 | 16.130 | 16.027 | 15.891 | 15.724 |
| | $\lambda_4^{M2x}$ | 17.618 | 17.294 | 16.943 | 16.573 | 16.189 | 15.795 | 15.399 | 15.112 | 15.087 |
| BC3 | $\lambda_1^{M2s}$ | 10.275 | 10.355 | 10.400 | 10.416 | 10.388 | 10.379 | 10.331 | 10.266 | 10.186 |
| | $\lambda_1^{M2x}$ | 10.272 | 10.286 | 10.305 | 10.339 | 10.392 | 10.427 | 10.487 | 10.553 | 10.645 |
| | $\lambda_2^{M2s}$ | 11.485 | 11.682 | 11.880 | 12.081 | 12.247 | 12.499 | 12.719 | 12.951 | 13.193 |
| | $\lambda_2^{M2x}$ | 10.835 | 11.195 | 11.552 | 11.899 | 12.242 | 12.581 | 12.937 | 13.272 | 13.626 |
| | $\lambda_3^{M2s}$ | 16.656 | 16.794 | 16.869 | 16.892 | 16.869 | 16.806 | 16.707 | 16.574 | 16.410 |
| | $\lambda_3^{M2x}$ | 16.705 | 16.959 | 17.183 | 17.397 | 16.872 | 16.734 | 16.375 | 16.011 | 15.658 |
| | $\lambda_4^{M2s}$ | 17.548 | 17.650 | 17.714 | 17.748 | 17.757 | 17.745 | 17.712 | 17.663 | 17.598 |
| | $\lambda_4^{M2x}$ | 18.719 | 18.386 | 18.029 | 17.653 | 17.748 | 17.947 | 18.126 | 18.293 | 18.443 |

$$\lambda_i = \omega_i a^2 \sqrt{\rho h_0 / D_{11}}, D_{11} = \frac{E_1 h_0^3}{12\left(1 - \vartheta_{21}\vartheta_{12}\right)}$$

**Table 10:** Variation of natural frequency parameter for M2x and M2s models

Tables 9 to 11 show the variation of frequency parameter against thickness parameter for circular cylindrical shells, when their boundary conditions are of BC2 or BC3 types. In comparison with the results explained for the case of the BC1 boundary condition, the frequency parameter varies at the same manner against thickness parameter for the models having variable thickness along their axis and the models having variable thickness along their circumference, when the boundary conditions are of either BC2 or BC3 types.

From the results summarized in Tables 9 to 11, it is observed that with increase in the value of C/b for the models, frequency parameter is also increased.

| Model ID: M3 | | | | | | $\alpha$ | | | | |
|---|---|---|---|---|---|---|---|---|---|---|
| Boundary Conditions | $\lambda$ | -0.4 | -0.3 | -0.2 | -0.1 | 0 | 0.1 | 0.2 | 0.3 | 0.4 |
| BC1 | $\lambda_1^{M3s}$ | 16.878 | 16.840 | 16.799 | 16.752 | 16.701 | 16.644 | 16.578 | 16.504 | 16.421 |
| | $\lambda_1^{M3x}$ | 16.195 | 16.324 | 16.448 | 16.572 | 16.696 | 16.823 | 16.952 | 17.084 | 17.217 |
| | $\lambda_2^{M3s}$ | 18.305 | 18.658 | 18.972 | 19.246 | 19.543 | 19.684 | 19.850 | 19.981 | 20.077 |
| | $\lambda_2^{M3x}$ | 21.196 | 20.890 | 20.583 | 20.219 | 19.565 | 19.507 | 19.146 | 18.789 | 18.440 |
| | $\lambda_3^{M3s}$ | 25.817 | 25.876 | 25.909 | 25.916 | 25.908 | 25.855 | 25.787 | 25.520 | 25.219 |
| | $\lambda_3^{M3x}$ | 25.337 | 25.608 | 25.816 | 25.909 | 25.939 | 25.998 | 25.999 | 25.976 | 25.930 |
| | $\lambda_4^{M3s}$ | 26.981 | 26.855 | 26.694 | 26.506 | 26.242 | 26.056 | 25.799 | 25.692 | 25.57 |
| | $\lambda_4^{M3x}$ | 25.506 | 25.683 | 25.843 | 26.044 | 26.248 | 26.364 | 26.483 | 26.577 | 26.644 |
| BC2 | $\lambda_1^{M3s}$ | 10.042 | 10.120 | 10.167 | 10.188 | 10.187 | 10.166 | 10.129 | 10.078 | 10.013 |
| | $\lambda_1^{M3x}$ | 10.283 | 10.258 | 10.233 | 10.210 | 10.190 | 10.177 | 10.173 | 10.177 | 10.193 |
| | $\lambda_2^{M3s}$ | 13.985 | 14.277 | 14.547 | 14.790 | 14.996 | 15.145 | 15.217 | 15.204 | 15.118 |
| | $\lambda_2^{M3x}$ | 13.883 | 14.271 | 14.619 | 14.917 | 15.129 | 15.181 | 15.047 | 14.806 | 14.525 |
| | $\lambda_3^{M3s}$ | 15.761 | 15.927 | 16.042 | 16.124 | 16.195 | 16.282 | 16.411 | 16.593 | 16.822 |
| | $\lambda_3^{M3x}$ | 17.555 | 17.248 | 16.942 | 16.663 | 16.182 | 16.391 | 16.512 | 16.741 | 17.017 |
| | $\lambda_4^{M3s}$ | 18.787 | 18.952 | 19.076 | 19.166 | 19.230 | 19.265 | 19.280 | 19.276 | 19.251 |
| | $\lambda_4^{M3x}$ | 18.696 | 18.893 | 19.043 | 19.154 | 19.233 | 19.283 | 19.308 | 19.311 | 19.292 |
| BC3 | $\lambda_1^{M3s}$ | 11.767 | 11.862 | 11.923 | 11.956 | 11.966 | 11.954 | 11.924 | 11.877 | 11.815 |
| | $\lambda_1^{M3x}$ | 11.471 | 11.535 | 11.674 | 11.818 | 11.970 | 12.132 | 12.304 | 12.490 | 12.690 |
| | $\lambda_2^{M3s}$ | 15.450 | 15.679 | 15.882 | 16.047 | 16.162 | 16.217 | 16.211 | 16.152 | 16.047 |
| | $\lambda_2^{M3x}$ | 14.762 | 15.266 | 15.727 | 16.121 | 16.260 | 16.343 | 16.154 | 15.905 | 15.578 |
| | $\lambda_3^{M3s}$ | 16.603 | 16.810 | 16.982 | 17.143 | 17.475 | 17.515 | 17.749 | 18.015 | 18.308 |
| | $\lambda_3^{M3x}$ | 18.291 | 18.030 | 17.777 | 17.569 | 17.503 | 17.688 | 18.047 | 18.475 | 18.934 |
| | $\lambda_4^{M3s}$ | 20.960 | 21.111 | 21.216 | 21.285 | 21.321 | 21.331 | 21.315 | 21.276 | 21.214 |
| | $\lambda_4^{M3x}$ | 20.012 | 20.383 | 20.721 | 21.034 | 21.324 | 21.595 | 21.849 | 22.089 | 22.316 |

$$\lambda_i = \omega_i a^2 \sqrt{\rho h_0 / D_{11}}, D_{11} = \frac{E_1 h_0^3}{12\left(1 - \vartheta_{21}\vartheta_{12}\right)}$$

**Table 11:** Variation of natural frequency parameter for M3x and M3s models.

In Tables 12 to 14, variation of frequency parameter against thickness parameter (α), for parabolic models is presented. Similar to the results for circular models, it is observed herein also that with any increase in the value of C/b for the models with parabolic profile, frequency parameter increases. The tendencies of the variation of frequency parameter for the models having parabolic profile are the same as those for the models having circular profile. Nevertheless, frequency parameter for the parabolic models is greater than that for the circular models, as confirmed also in Cheung and Cheung (1972).

| Model ID: M4 | | | | | | $\alpha$ | | | | |
|---|---|---|---|---|---|---|---|---|---|---|
| Boundary Conditions | λ | -0.4 | -0.3 | -0.2 | -0.1 | 0 | 0.1 | 0.2 | 0.3 | 0.4 |
| BC1 | $\lambda_1^{M4s}$ | 12.295 | 12.545 | 12.771 | 12.973 | 13.151 | 13.308 | 13.471 | 13.556 | 13.648 |
| | $\lambda_1^{M4x}$ | 14.111 | 13.908 | 13.696 | 13.480 | 13.181 | 13.044 | 12.649 | 12.620 | 12.416 |
| | $\lambda_2^{M4s}$ | 13.787 | 13.960 | 14.114 | 14.356 | 14.836 | 14.884 | 14.946 | 15.011 | 15.250 |
| | $\lambda_2^{M4x}$ | 14.974 | 14.955 | 14.933 | 14.908 | 14.878 | 14.843 | 14.723 | 14.746 | 14.680 |
| | $\lambda_3^{M4s}$ | 18.108 | 18.206 | 18.274 | 18.315 | 18.227 | 18.089 | 17.923 | 17.816 | 17.683 |
| | $\lambda_3^{M4x}$ | 17.596 | 17.767 | 17.921 | 18.059 | 18.211 | 18.289 | 18.363 | 18.382 | 18.353 |
| | $\lambda_4^{M4s}$ | 18.744 | 18.626 | 18.498 | 18.364 | 18.339 | 18.318 | 18.256 | 18.224 | 18.141 |
| | $\lambda_4^{M4x}$ | 17.931 | 18.080 | 18.195 | 18.288 | 18.342 | 18.377 | 18.403 | 18.462 | 18.525 |
| BC2 | $\lambda_1^{M4s}$ | 5.927 | 6.026 | 6.120 | 6.215 | 6.309 | 6.405 | 6.486 | 6.606 | 6.7155 |
| | $\lambda_1^{M4x}$ | 5.8735 | 5.990 | 6.099 | 6.205 | 6.308 | 6.409 | 6.451 | 6.615 | 6.720 |
| | $\lambda_2^{M4s}$ | 8.336 | 8.405 | 8.437 | 8.436 | 8.418 | 8.356 | 8.245 | 8.191 | 8.081 |
| | $\lambda_2^{M4x}$ | 9.043 | 8.896 | 8.748 | 8.602 | 8.441 | 8.324 | 8.142 | 8.076 | 7.966 |
| | $\lambda_3^{M4s}$ | 12.297 | 12.343 | 12.387 | 12.432 | 12.477 | 12.529 | 12.526 | 12.511 | 12.459 |
| | $\lambda_3^{M4x}$ | 12.121 | 12.255 | 12.349 | 12.411 | 12.445 | 12.456 | 12.420 | 12.414 | 12.365 |
| | $\lambda_4^{M4s}$ | 12.523 | 12.592 | 12.630 | 12.643 | 12.636 | 12.611 | 12.646 | 12.653 | 12.729 |
| | $\lambda_4^{M4x}$ | 12.526 | 12.590 | 12.627 | 12.644 | 12.644 | 12.630 | 12.591 | 12.570 | 12.528 |
| BC3 | $\lambda_1^{M4s}$ | 7.432 | 7.467 | 7.504 | 7.545 | 7.592 | 7.645 | 7.685 | 7.777 | 7.859 |
| | $\lambda_1^{M4x}$ | 6.633 | 6.861 | 7.086 | 7.309 | 7.592 | 7.756 | 7.871 | 8.209 | 8.440 |
| | $\lambda_2^{M4s}$ | 9.266 | 9.328 | 9.355 | 9.350 | 9.321 | 9.270 | 9.184 | 9.109 | 9.005 |
| | $\lambda_2^{M4x}$ | 9.666 | 9.587 | 9.508 | 9.432 | 9.359 | 9.290 | 9.229 | 9.170 | 9.122 |
| | $\lambda_3^{M4s}$ | 15.033 | 15.084 | 15.102 | 15.095 | 15.025 | 14.944 | 14.885 | 14.798 | 14.736 |
| | $\lambda_3^{M4x}$ | 13.705 | 14.000 | 14.271 | 14.520 | 14.999 | 15.061 | 15.269 | 15.335 | 15.413 |
| | $\lambda_4^{M4s}$ | 15.310 | 15.254 | 15.183 | 15.105 | 15.065 | 15.021 | 14.913 | 14.879 | 14.790 |
| | $\lambda_4^{M4x}$ | 14.305 | 14.528 | 14.722 | 14.890 | 15.036 | 15.160 | 15.312 | 15.347 | 15.498 |

$$\lambda_i = \omega_i a^2 \sqrt{\rho h_0 / D_{11}}, D_{11} = \frac{E_1 h_0^3}{12\left(1-\vartheta_{21}\vartheta_{12}\right)}$$

**Table 12:** Variation of natural frequency parameter for M4x and M4s models.

| Model ID:M5 | | α | | | | | | | | |
|---|---|---|---|---|---|---|---|---|---|---|
| Boundary Conditions | λ | -0.4 | -0.3 | -0.2 | -0.1 | 0 | 0.1 | 0.2 | 0.3 | 0.4 |
| BC1 | $\lambda_1^{M5s}$ | 14.838 | 14.956 | 15.063 | 15.169 | 15.254 | 15.322 | 15.414 | 15.438 | 15.465 |
| | $\lambda_1^{M5x}$ | 15.471 | 15.413 | 15.348 | 15.286 | 15.234 | 15.187 | 15.153 | 15.123 | 15.115 |
| | $\lambda_2^{M5s}$ | 19.295 | 19.795 | 19.966 | 20.042 | 20.066 | 20.641 | 21.047 | 21.272 | 21.463 |
| | $\lambda_2^{M5x}$ | 20.839 | 21.014 | 20.798 | 20.443 | 20.062 | 19.668 | 19.325 | 18.822 | 18.383 |
| | $\lambda_3^{M5s}$ | 22.732 | 22.728 | 22.652 | 22.586 | 22.494 | 22.389 | 22.311 | 22.17 | 21.939 |
| | $\lambda_3^{M5x}$ | 20.416 | 20.123 | 20.169 | 20.615 | 20.962 | 21.515 | 21.593 | 21.673 | 21.736 |
| | $\lambda_4^{M5s}$ | 25.254 | 25.381 | 25.477 | 25.535 | 25.571 | 25.583 | 25.549 | 25.534 | 25.456 |
| | $\lambda_4^{M5x}$ | 25.320 | 25.451 | 25.535 | 25.575 | 25.577 | 25.541 | 25.470 | 25.366 | 25.227 |
| BC2 | $\lambda_1^{M5s}$ | 9.595 | 9.6724 | 9.714 | 9.726 | 9.714 | 9.680 | 9.575 | 9.556 | 9.4718 |
| | $\lambda_1^{M5x}$ | 10.071 | 9.985 | 9.882 | 9.794 | 9.7235 | 9.639 | 9.5134 | 9.513 | 9.466 |
| | $\lambda_2^{M5s}$ | 10.942 | 11.183 | 11.415 | 11.641 | 11.864 | 12.086 | 12.237 | 12.533 | 12.758 |
| | $\lambda_2^{M5x}$ | 10.846 | 11.118 | 11.362 | 11.617 | 11.841 | 12.073 | 12.419 | 12.527 | 12.745 |
| | $\lambda_3^{M5s}$ | 15.635 | 15.756 | 15.842 | 15.900 | 15.934 | 15.950 | 15.943 | 15.931 | 15.900 |
| | $\lambda_3^{M5x}$ | 15.616 | 15.739 | 15.822 | 15.884 | 15.920 | 15.948 | 15.945 | 15.937 | 15.772 |
| | $\lambda_4^{M5s}$ | 16.668 | 16.805 | 16.880 | 16.902 | 16.880 | 16.818 | 16.633 | 16.593 | 16.436 |
| | $\lambda_4^{M5x}$ | 18.323 | 17.999 | 17.648 | 17.275 | 16.887 | 16.487 | 16.081 | 15.672 | 15.471 |
| BC3 | $\lambda_1^{M5s}$ | 10.864 | 10.944 | 10.992 | 11.007 | 10.999 | 10.970 | 10.902 | 10.858 | 10.778 |
| | $\lambda_1^{M5x}$ | 10.941 | 10.946 | 10.954 | 10.965 | 10.991 | 11.022 | 11.075 | 11.123 | 11.197 |
| | $\lambda_2^{M5s}$ | 12.297 | 12.502 | 12.706 | 12.912 | 13.123 | 13.340 | 13.593 | 13.798 | 14.041 |
| | $\lambda_2^{M5x}$ | 11.687 | 12.052 | 12.406 | 12.761 | 13.119 | 13.450 | 13.831 | 14.155 | 14.574 |
| | $\lambda_3^{M5s}$ | 17.336 | 17.471 | 17.543 | 17.565 | 17.543 | 17.481 | 17.397 | 17.255 | 17.339 |
| | $\lambda_3^{M5x}$ | 17.288 | 17.523 | 17.754 | 17.971 | 17.543 | 17.269 | 17.059 | 16.754 | 16.376 |
| | $\lambda_4^{M5s}$ | 17.966 | 18.070 | 18.137 | 18.175 | 18.188 | 18.181 | 18.136 | 18.111 | 18.053 |
| | $\lambda_4^{M5x}$ | 19.295 | 18.992 | 18.629 | 18.246 | 18.197 | 18.280 | 18.454 | 18.614 | 18.758 |

$$\lambda_i = \omega_i a^2 \sqrt{\rho h_0 / D_{11}}, D_{11} = \frac{E_1 h_0^3}{12\left(1 - \vartheta_{21}\vartheta_{12}\right)}$$

**Table 13:** Variation of natural frequency parameter for M5x and M5s models.

| Model: M6 | | $\alpha$ | | | | | | | | |
|---|---|---|---|---|---|---|---|---|---|---|
| Boundary conditions | $\lambda$ | -0.4 | -0.3 | -0.2 | -0.1 | 0 | 0.1 | 0.2 | 0.3 | 0.4 |
| B.c1 | $\lambda_1^{M6s}$ | 17.763 | 17.532 | 17.202 | 17.103 | 17.023 | 17.026 | 17.022 | 17.011 | 16.994 |
| | $\lambda_1^{M6x}$ | 16.670 | 16.761 | 16.850 | 16.941 | 17.037 | 17.140 | 17.251 | 17.321 | 17.501 |
| | $\lambda_2^{M6s}$ | 20.153 | 20.505 | 20.846 | 21.126 | 21.364 | 21.563 | 21.721 | 21.840 | 21.921 |
| | $\lambda_2^{M6x}$ | 23.397 | 23.046 | 22.666 | 22.265 | 21.350 | 21.126 | 20.998 | 20.577 | 20.150 |
| | $\lambda_3^{M6s}$ | 26.854 | 26.762 | 26.646 | 26.507 | 26.346 | 26.167 | 25.966 | 25.748 | 25.505 |
| | $\lambda_3^{M6x}$ | 25.442 | 25.715 | 25.956 | 26.170 | 26.360 | 26.528 | 26.675 | 26.806 | 26.914 |
| | $\lambda_4^{M6s}$ | 27.292 | 27.415 | 27.502 | 27.555 | 27.575 | 27.562 | 27.511 | 27.440 | 27.328 |
| | $\lambda_4^{M6x}$ | 27.429 | 27.588 | 27.696 | 27.759 | 27.783 | 27.772 | 27.730 | 27.668 | 27.564 |
| B.c2 | $\lambda_1^{M6s}$ | 10.611 | 10.694 | 10.745 | 10.768 | 10.770 | 10.752 | 10.718 | 10.668 | 10.605 |
| | $\lambda_1^{M6x}$ | 10.929 | 10.887 | 10.846 | 10.808 | 10.774 | 10.746 | 10.727 | 10.717 | 10.717 |
| | $\lambda_2^{M6s}$ | 15.480 | 15.823 | 16.136 | 16.364 | 16.511 | 16.361 | 16.263 | 16.129 | 15.962 |
| | $\lambda_2^{M6x}$ | 15.225 | 15.644 | 16.035 | 16.397 | 16.553 | 16.479 | 16.145 | 15.803 | 15.464 |
| | $\lambda_3^{M6s}$ | 16.315 | 16.447 | 16.536 | 16.652 | 16.960 | 17.203 | 17.521 | 17.845 | 18.177 |
| | $\lambda_3^{M6x}$ | 18.269 | 17.945 | 17.608 | 17.274 | 17.019 | 17.195 | 17.519 | 17.852 | 18.185 |
| | $\lambda_4^{M6s}$ | 18.622 | 18.799 | 18.937 | 19.041 | 19.119 | 19.174 | 19.208 | 19.223 | 19.221 |
| | $\lambda_4^{M6x}$ | 18.644 | 18.822 | 18.956 | 19.054 | 19.122 | 19.164 | 19.183 | 19.182 | 19.162 |
| B.c3 | $\lambda_1^{M6s}$ | 12.229 | 12.325 | 12.389 | 12.424 | 12.435 | 12.426 | 12.399 | 12.355 | 12.296 |
| | $\lambda_1^{M6x}$ | 11.974 | 12.084 | 12.195 | 12.313 | 12.439 | 12.574 | 12.721 | 12.879 | 13.052 |
| | $\lambda_2^{M6s}$ | 16.651 | 16.942 | 17.157 | 17.270 | 17.394 | 17.256 | 17.172 | 17.052 | 16.899 |
| | $\lambda_2^{M6x}$ | 16.111 | 16.645 | 17.146 | 17.353 | 17.444 | 17.347 | 17.039 | 16.725 | 16.417 |
| | $\lambda_3^{M6s}$ | 17.419 | 17.577 | 17.749 | 17.977 | 18.283 | 18.567 | 18.897 | 19.246 | 19.611 |
| | $\lambda_3^{M6x}$ | 18.991 | 18.706 | 18.417 | 18.177 | 18.309 | 18.743 | 19.218 | 19.705 | 20.200 |
| | $\lambda_4^{M6s}$ | 20.807 | 20.975 | 21.099 | 21.189 | 21.248 | 21.281 | 21.292 | 21.281 | 21.250 |
| | $\lambda_4^{M6x}$ | 20.013 | 20.364 | 20.683 | 20.977 | 21.248 | 21.501 | 21.736 | 21.957 | 22.163 |

$$\lambda_i = \omega_i a^2 \sqrt{\rho h_0 / D_{11}}, D_{11} = \frac{E_1 h_0^3}{12\left(1-\vartheta_{21}\vartheta_{12}\right)}$$

**Table 14:** Variation of natural frequency parameter for M6x and M6s models.

From the obtained numerical results, the following observations can be summarized:

- With increase in C/b (b is constant and C varies), frequency of all models (circular and parabolic profiles) is increased. With increase in C/b, arc length of both profiles will increase, and then weight of models increases. In addition, the increase of camber (C) will decrease radius of curvature of shells. Increase in the weight of the models decreases the natural frequency and also decrease of the radius of curvature increases the natural frequency of models. Therefore, effect of the change in the curvature on the natural frequency is greater than the effect of change in the weight for studied models. The tendencies of variation of frequency parameter are the same for both circular and parabolic models. Nevertheless, for the models with the same values of C/b, the natural frequency in case of parabolic curvature is greater than that in case of circular curvature. This phenomenon may be due to the facts that; (1) local stiffness of parabolic models is greater than local stiffness of circular models and (2) weight of circular models is greater than parabolic models with the same C/b (because the arc length of circular profile is greater than the arc length of parabolic profile).
- Effect of thickness variation along both directions on the natural frequency is studied. It was aimed to find out the difference between effect of thickness variation along direction with zero curvature (x direction) and effect of thickness variation along direction with nonzero curvature (s direction). It is observed that for the case of BC1 boundary condition, the frequency parameter variation for the models with variable thickness along their axis is in opposite tendency compared with the models having variable thickness along their circumference.
- Effect of boundary condition on natural frequency is studied for three cases. It can be seen that the effect of boundary condition on natural frequency is greater than the effect of variable thickness on natural frequency. Models with BC1 boundary condition have largest natural frequency and models with BC2 boundary condition have lowest natural frequency. In addition, boundary condition changes the manner of frequency parameter variation against the thickness parameter. For example, for the BC1 type of boundary condition, frequency parameter varies linearly against thickness parameter but for the BC2 and BC3 types of boundary condition, frequency parameter varies nonlinearly against thickness parameter.

### 3.3 Effect of variable thickness on the mode shapes

Eigen vectors of the Equation 13 are unknown coefficients of the displacement functions. By finding these unknown coefficients, the relevant mode shapes can be plotted. The effect of thickness parameter on the first four mode shapes is studied herein for the models M5s and M5x (both models have parabolic profiles). Figure 3 shows the effect of thickness parameter on the first four mode shapes for the model M5x (the parabolic cylindrical shell with variable thickness along x axis). In general, for the first and third modes, the mode shapes visually are similar to each others for different values of the thickness parameter. For negative (-) and positive (+) values of the thickness parameter ($\alpha$), the second and fourth modes have equal numbers of half waves but the way the half waves are appeared is opposite. Figure 4 shows the effect of thickness parameter on the mode shapes for the M5s

model (the parabolic cylindrical shell with variable thickness along s axis). As can be observed, the thickness parameter does not have any significant effect on the mode shape for M5s model.

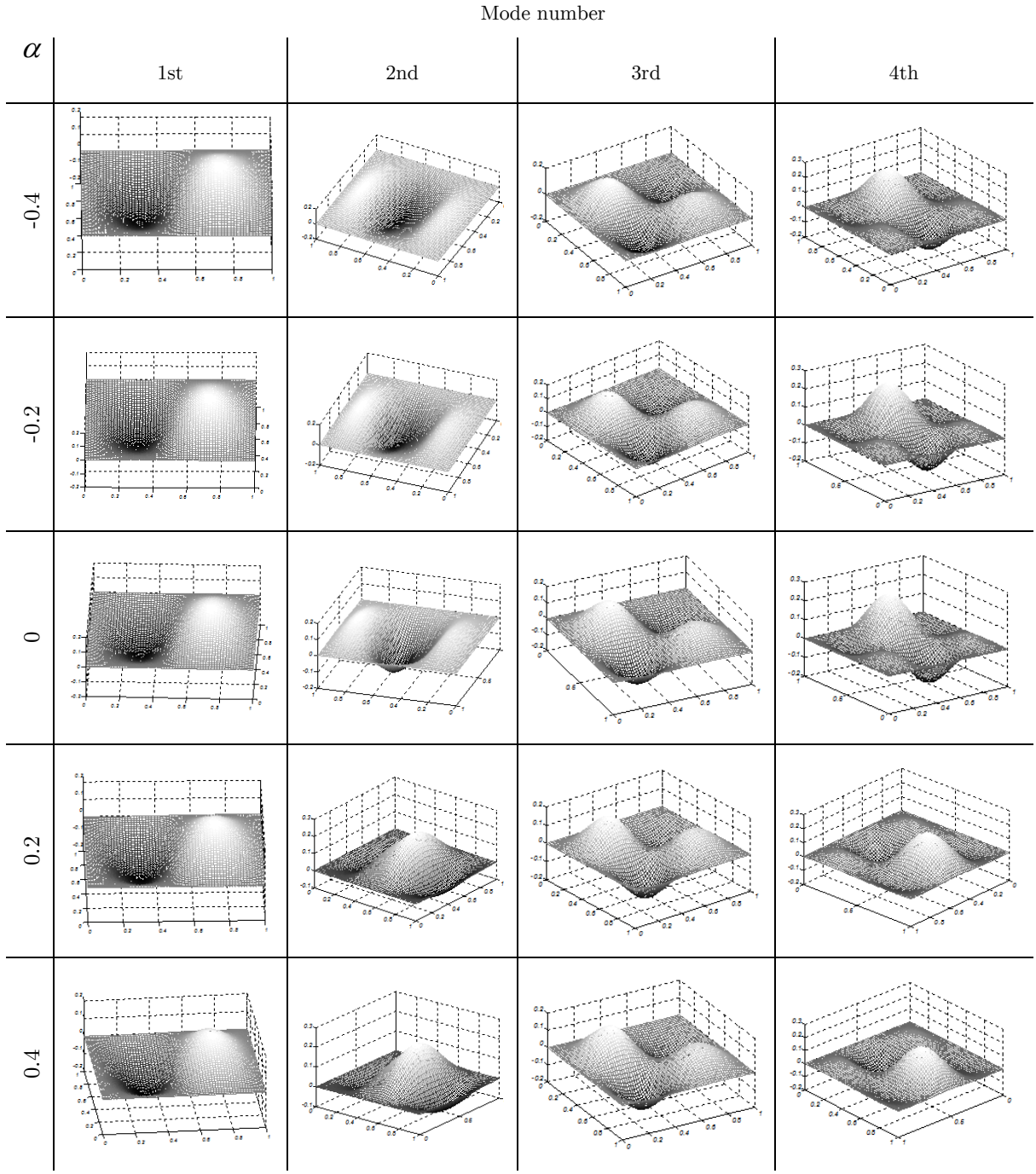


**Figure 3:** Effect of thickness parameter ($\alpha$) on the mode shapes for the parabolic model with $^{c}/_{b} = 0.15$ (Model M6s).

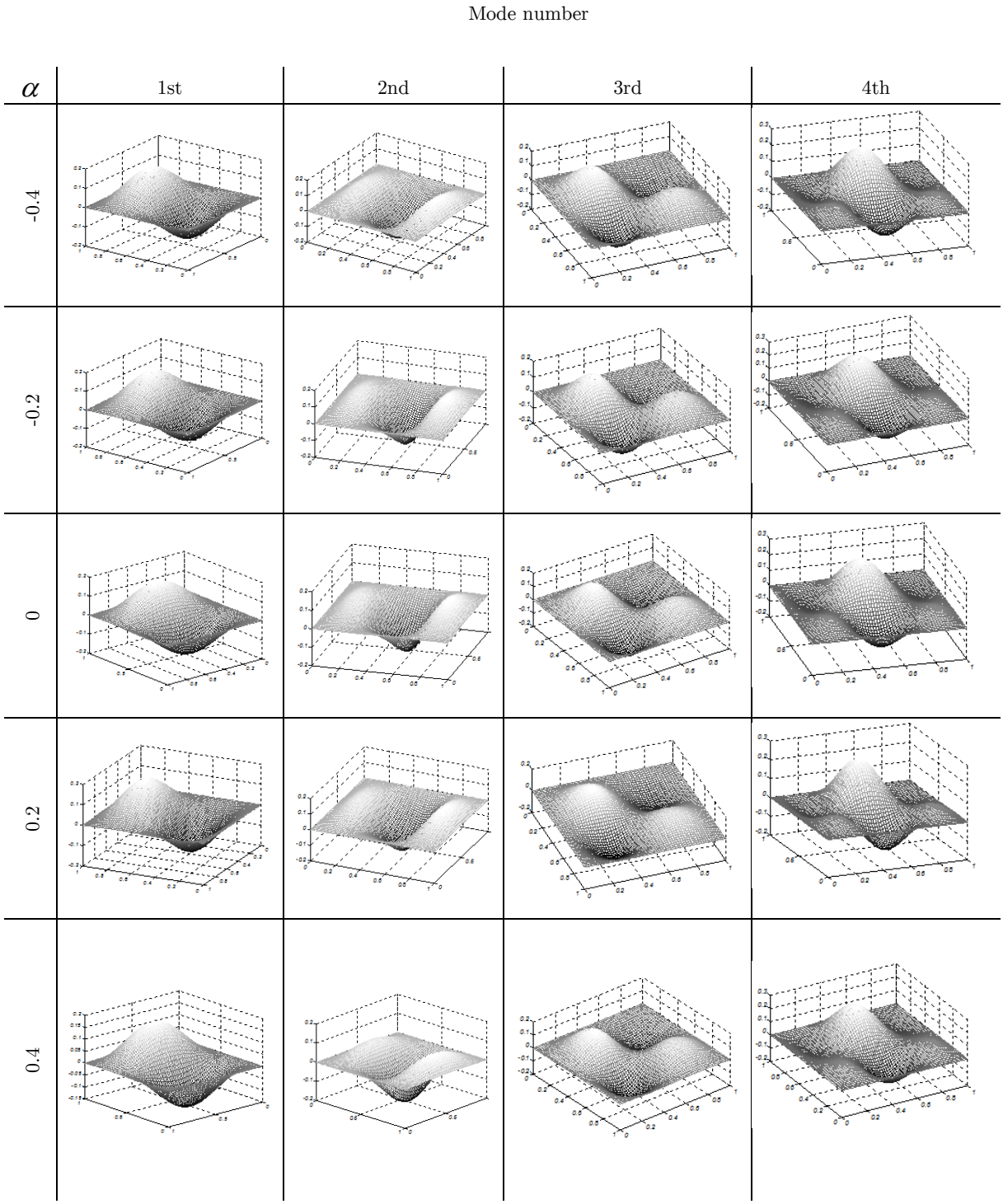


**Figure 4:** Effect of thickness parameter ($\alpha$) on the mode shapes for the parabolic model with $^{c}/_{b} = 0.15$ (Model M6x).

## 4 CONCLUSIONS

An approximate analysis method for investigating the free vibration behavior of circular and parabolic cylindrical shells having variable thickness along their axis or circumference is presented. A finite element method based on B-spline functions is further extended to find out the natural frequencies and corresponding mode shapes for the cylindrical shells with variable radii of curvature and non-uniform thicknesses. Usefulness and accuracy of the present method is demonstrated through comparison of the results for a variety of cases. It is observed that frequency parameter for circular models vary in the same way against thickness parameter as that for parabolic models. Moreover, natural frequency of cylindrical models with a parabolic profile is slightly greater than that of cylindrical models with a circular profile.

### References

Ashour, A.S., (2001). A semi-analytical solution of the flexural vibration of orthotropic plates of variable thickness, Journal of Sound and Vibration 240: 431–445.

Cheng, S.P., Chuang, D., (1990). Dynamic analysis of stiffened plates and shells using spline gauss collocation method, Computers & Structures 36: 623-629.

Cheng, S.P., Dade, H., Zongmu, W., (1987). Static, vibration and stability analysis of stiffened plates using B spline functions, Computers & Structures27:73-78.

Cheung, Y. K., Cheung, M.S., (1972). Vibration analysis of cylindrical panels, Journal of Sound and Vibration 22: 59-73.

Duan, W., Koh, C., (2008). Axisymmetric transverse vibrations of circular cylindrical shells with variable thickness, Journal of Sound and Vibration 317: 1035–1041.

Grigorenko, A.Y., Parkhomenko, A.Y., (2011). Free Vibration of Shallow Orthotropic Shells with Variable Thickness and Rectangular platform, Journal of International Applied Mechanics 46: 877-889.

Grigorenko, Y.M., Grigorenko, A.Y., Efimova, T.L., (2008). Spline-based investigation of natural vibrations of orthotropic rectangular plates of variable thickness within classical and refined theories, Journal of Mechanics of Materials and Structures 3: 929-952.

Huang, M., Ma, X.Q., Sakiyama, T., Matsuda, H., Morita, C., (2005). Free vibration analysis of orthotropic rectangular plates with variable thickness and general boundary conditions, Journal of Sound and Vibration 288: 931-955.

Huang, M., Ma, X.Q., Sakiyama, T., Matsuda, H., Morita, C., (2007). Free vibration analysis of rectangular plates with variable thickness and point supports, Journal of Sound and Vibration 300: 435-452.

Khalifa, A.M., (2011). Simplified equations and solutions for the free vibration of an orthotropic oval cylindrical shell with variable thickness, Math. Meth. Appl. Sci 34: 1789-1800.

Pellicano, F., (2007). Vibrations of circular cylindrical shells: theory and experiments, Journal of Sound and Vibration 303: 154–170.

Sakiyama, T., Huang, M., (1998). Free vibration analysis of rectangular plates with variable thickness, Journal of Sound and Vibration 216: 379–397.

Sivadas, K., Ganesan, N., (1991). Free vibration of circular cylindrical shells with axially varying thickness, Journal of Sound and Vibration 147: 73–85.

Soedel, W. (1993). Vibration of Shells and plates, Marcel Dekker INC.

Srinivasan, R.S., Bobby, W., (1976). Free vibration of noncircular cylindrical shell panels, Journal of Sound and Vibration 46: 43-49.

Suzuki, K., Leissa, A., (1985).Free vibrations of noncircular cylindrical shells having circumferentially varying thickness, Journal of Applied Mechanics52: 149–154.

Yamada, G., Irie, T., Notoya, S., (1999). Natural frequencies of elliptical cylindrical shells, Journal of Sound and Vibration 101: 133–139.

Zhang, L., Xiang, Y., (2006). Exact solutions for vibration of stepped circular cylindrical shells, Journal of Sound and Vibration 299: 948–964.

Zhang, X., Liu, G., Lam, K., (2001). Vibration analysis of thin cylindrical shells using wave propagation approach, Journal of Sound and Vibration 239: 397–403.